

HORIZON WAVE-FUNCTION: FROM PARTICLES TO BLACK HOLES

ROBERTO CASADIO¹, OCTAVIAN MICU², FABIO SCARDIGLI^{3,4}

¹ Dipartimento di Fisica e Astronomia, Università di Bologna,
via Irnerio 46, I-40126 Bologna, Italy,
Email: *casadio@bo.infn.it*

² Institute of Space Science,
Atomistilor 409, RO-077125, Măgurele-Bucharest, Romania,
Email: *octavian.micu@spacescience.ro*

³ Dipartimento di Matematica, Politecnico di Milano,
Piazza L. da Vinci 32, 20133 Milano, Italy,

⁴ Yukawa Institute for Theoretical Physics, Kyoto University,
Kyoto 606-8502, Japan,
Email: *fabio@phys.ntu.edu.tw*

Received July 5, 2015

Abstract. Localised Quantum Mechanical particles are described by wave packets in position space, regardless of their energy. From a General Relativistic point of view, when a particle's energy density is larger than a certain threshold, the particle should be a black hole. We combine these two pictures by introducing a horizon wave-function determined by the particle wave-function in position space, which is used to compute the probability that the particle is a black hole. The sources are modelled as simple Gaussian wave-packets and using the horizon wave-function formalism we calculate the probability for these particles to be Schwarzschild black holes, respectively Reissner-Nordstrom black holes (in the case of charged particles). We also derive an effective Generalised Uncertainty Principle (GUP), which is obtained by adding the uncertainties coming from the two wave-functions associated to the particle.

Key words: Horizon wave-function, black holes, Planck scale, Gaussian wave-packets, generalised uncertainty principle.

PACS: 04.70.Dy, 04.70.-s, 04.60.-m

1. INTRODUCTION

Our present understanding of the Universe relies on two theories: the theory of General Relativity which is applicable at very large scales, and Quantum Mechanics (QM) which is a very good description of the microscopic universe. While these two theories work very well, each in its own regime, one regime in which they collide is near the Planck scale, when QM wave-packets can turn into Black Holes (BH). Another interesting problem is the description of the gravitational collapse which again leads to the formation of BHs (first investigated in the seminal papers of Oppenheimer and co-workers [1, 2]). A lot of work has been done on this subject, but

a good description of the physics of such processes is still challenging. There is a vast amount of literature on this subject (see, e.g. Ref. [3]), but many technical and conceptual difficulties remain unsolved, such as accounting for the QM nature of collapsing matter.

Until now, the only unanimously accepted idea is that gravitation becomes important whenever a large enough amount of matter is “compact” within a sufficiently small volume. K. Thorne formulated this idea in the *hoop conjecture* [4], which states that a BH forms when two colliding objects fall within their “black disk”. Assuming the final configuration is (approximately) spherically symmetric, this occurs when the system occupies a sphere whose radius r is smaller than the gravitational Schwarzschild radius,

$$r \lesssim R_H \equiv 2 \ell_p \frac{E}{m_p}, \quad (1)$$

where the Planck length is denoted by ℓ_p and m_p represents the Planck mass.*

One can find many attempts at quantising BH metrics in the literature, which focus on the purely gravitational degrees of freedom, and result in a description of the horizon which is unrelated to the matter state that sourced the geometry to begin with [5]. The approach discussed in this paper, the Horizon Wave Function (HWF) formalism [6–8], is instead based on the quantum version of the Einstein equations. It relates the size of the horizon to the (quantum) state of matter. When applied to several case studies [9–11], the results were found to be in agreement with (semi)classical expectations, which makes us hopeful that it will help further our understanding of the quantum nature of BHs.

The formalism starts from the spectral decomposition of the QM state that represents the matter source. The total energy is then written in terms of the gravitational radius, as it is classically determined from Einstein equations, and the spectral decomposition then yields the HWF. The normalized HWF is then used to compute the probability for an observer to find a horizon of a certain areal radius centered around that particular QM source.

Electrically charged BHs were subject to many theoretical studies in the past [12]. In Refs. [13, 14] we extend the HWF formalism to the Reissner-Nordström metric and investigated the probability for an electrically charged source represented by a Gaussian wave-packet to be a BH, and to have an actual inner horizon. These findings will be detailed in Section 2.2. The inner horizon is a Cauchy horizon and is associated with an instability known as “mass inflation”: any small matter perturbation will blue-shift unboundedly just outside this horizon and inevitably produce a large deformation to the background geometry [15], although the existence of this

*We use units with $c = k_B = 1$, and always display the Newton constant $G_N = \ell_p/m_p$, so that $\hbar = \ell_p m_p$.

effect is still debated (see, e.g. Refs. [16–18]). It is thus interesting to study under which conditions the inner horizon survives in the QM treatment.

2. THE HORIZON WAVE-FUNCTION FORMALISM

The formalism described in the section below was proposed fairly recently, and it already resulted in some very interesting findings. [7, 9, 13, 14]

We start with the wave-function ψ_S of a massive QM particle, which is localised in space and at rest in the chosen reference frame. In the present work we focus on particles that, for simplicity, we consider to be spherically symmetric. A simple example for such a source is the Gaussian wave-function

$$\psi_S(r) = \frac{e^{-\frac{r^2}{2\ell^2}}}{\ell^{3/2} \pi^{3/4}}, \quad (2)$$

of width ℓ assumed to be the minimum compatible with the Heisenberg uncertainty principle

$$\ell = \lambda_m \simeq \ell_p \frac{m_p}{m}. \quad (3)$$

Here λ_m is the Compton length of the particle of rest mass m .

The state can be expanded in Hamiltonian eigenmodes as

$$|\psi_S\rangle = \sum_E C(E) |\psi_E\rangle, \quad (4)$$

where the Hamiltonian is specified depending on the model we wish to consider.

One can then invert the expression of the Schwarzschild radius, represented by the identity from Eq. (1), to obtain the total energy E as a function of R_H , and use it to define the HWF as

$$\psi_H(R_H) \propto C(m_p R_H/2\ell_p), \quad (5)$$

whose normalisation is fixed in the inner product

$$\langle \psi_H | \phi_H \rangle = 4\pi \int_0^\infty \psi_H^*(R_H) \phi_H(R_H) R_H^2 dR_H. \quad (6)$$

We think of this normalised wave-function ψ_H simply as yielding the probability that one would detect a horizon of radius $r = R_H$ associated with the particle in the QM state ψ_S that we began with. Unlike general relativistic horizons, such a horizon is necessarily "fuzzy", like the position of the particle itself.

With the HWF at hand, one can proceed to calculate the probability density for the particle to lie inside its own horizon of radius $r = R_H$:

$$P_<(r < R_H) = P_S(r < R_H) P_H(R_H), \quad (7)$$

where

$$P_S(r < R_H) = 4\pi \int_0^{R_H} |\psi_S(r)|^2 r^2 dr \quad (8)$$

is the probability that the particle is inside a sphere of radius $r = R_H$, and

$$P_H(R_H) = 4\pi R_H^2 |\psi_H(R_H)|^2 \quad (9)$$

is the probability that the horizon is located on the sphere of radius $r = R_H$.

Finally, the probability that the particle described by the wave-function ψ_S is a BH will be obtained by integrating (15) over all possible values of the radius,

$$P_{BH} = \int_0^\infty P_<(r < R_H) dR_H. \quad (10)$$

The reader should keep in mind that depending on type of particle being taken into consideration, the space-time metric changes and in some cases more than one horizon exist. In Section 2.2 the results obtained in the case of electrically charged particles will be presented. Charged BHs are described by the Reissner-Nordström metric, which has two horizons: an exterior and an interior one.

2.1. NEUTRAL PARTICLES. SCHWARZSCHILD BLACK HOLES

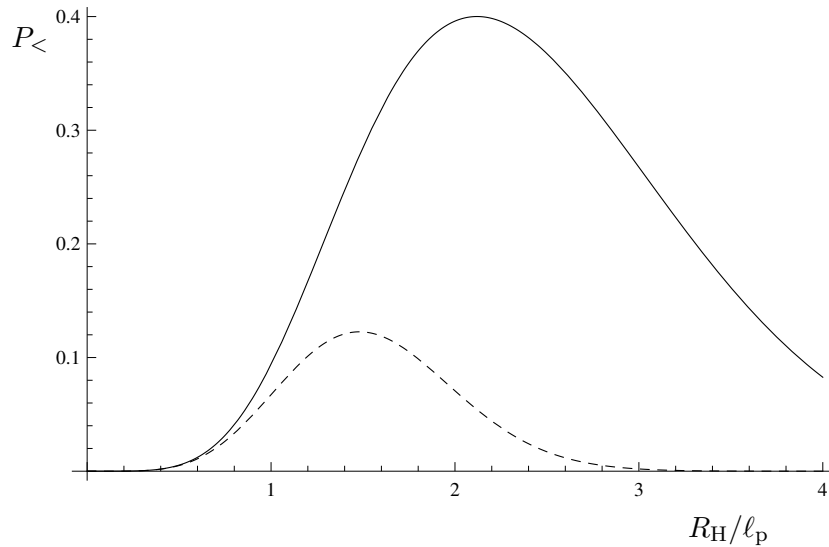


Fig. 1 – Probability density $P_<$ in Eq. (15) that particle is inside its horizon of radius $R = R_H$, for $\ell = \ell_p$ (solid line) and for $\ell = 2\ell_p$ (dashed line).

Figure 1 represents the probability density $P_<$ for the particle to be within its own radius $R = R_H$. The probability density is plotted for two values of the Gaussian

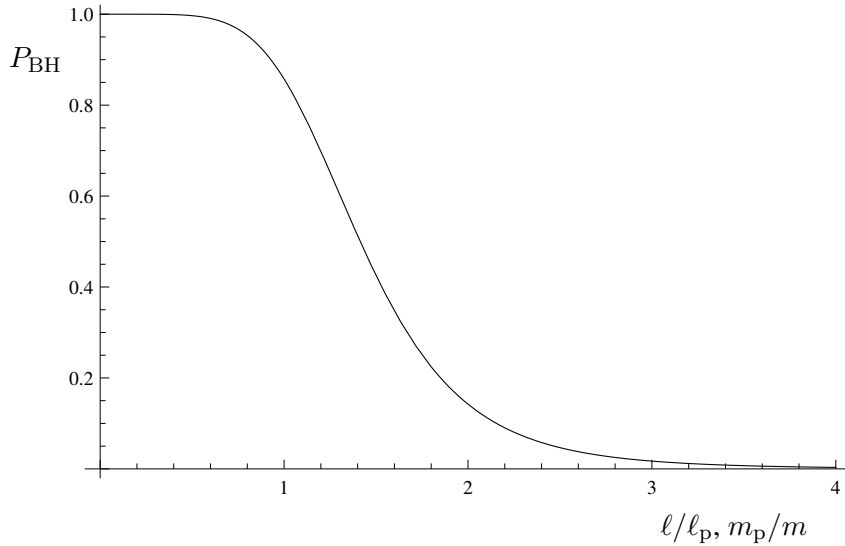


Fig. 2 – Probability P_{BH} in Eq. (10) that particle of width $\ell \sim m^{-1}$ is a BH.

width: $\ell = \ell_p$ and $\ell = 2\ell_p$. The reader is reminded that these values correspond to $m = m_p$ and $m = 0.5m_p$. The plot shows that, as expected, the probability density is larger for larger values of the particle mass (narrower spread of the wave-packet). One can integrate the probability density and calculate the probability P_{BH} for the particle/wave-packet to form a BH.

The probability P_{BH} is shown in Fig. 2 as a function of ℓ (in units of ℓ_p). One can see that the probability for the wave-packet to be a BH is equal to one for widths of the Gaussian smaller than the Planck length and that it decreases slowly until it becomes negligible for widths around $3\ell_p$. This behaviour, the fact that the probability decreases smoothly and is different from zero even for energies below the Planck mass is due to the quantum effects (otherwise, BH formation is a threshold effect which appears exactly at the Planck scale).

2.1.1. Effective GUP

For QM wave-packets near the Planck scale, such as the Gaussian packet considered herein, there are two sources of uncertainty. One is the standard QM uncertainty, and then there is the uncertainty in the localisation of the horizon radius (the complete details can be found in [7]). By linearly combining the two, we find

$$\begin{aligned} \Delta r &\equiv \sqrt{\langle \Delta r^2 \rangle} + \gamma \sqrt{\langle \Delta R_{\text{H}}^2 \rangle} \\ &= \left(\frac{3\pi - 8}{2\pi} \right) \ell_p \frac{m_p}{\Delta p} + 2\gamma \ell_p \frac{\Delta p}{m_p}, \end{aligned} \quad (11)$$

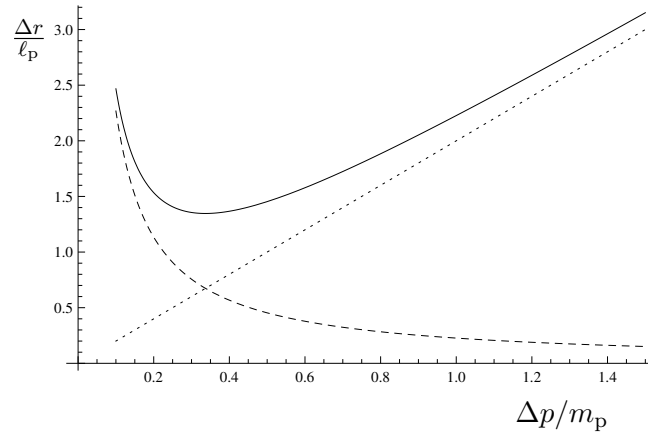


Fig. 3 – Uncertainty relation (11) (solid line) as a combination of the QM uncertainty (dashed line) and the uncertainty in horizon radius (dotted line).

where γ is a coefficient of order one. The result is plotted (for $\gamma = 1$) in Fig. 3, where it is also compared to the usual Heisenberg uncertainty in the position.

2.2. ELECTRICALLY CHARGED PARTICLES. REISSNER-NORDSTRÖM BLACK HOLES

Let us now turn our attention to the results obtained for charged particles, case in which the metric that describes the resulting BH is the Reissner-Nordström metric:

$$ds^2 = -f dt^2 + f^{-1} dr^2 + r^2 (d\theta^2 + \sin^2 \theta d\phi^2), \quad (12)$$

with

$$f = 1 - \frac{2\ell_p M}{m_p r} + \frac{Q^2}{r^2}, \quad (13)$$

where M represents the ADM mass and Q the charge of the source. The above BH metric contains two horizons, namely

$$R_{\pm} = \ell_p \frac{M}{m_p} \left(1 \pm \sqrt{1 - \alpha^2} \right), \quad (14)$$

where $\alpha = \frac{|Q|m_p}{\ell_p M}$ is the specific charge of the BH. These classical relations are lifted to the rank of equations for the operators \hat{R}_{\pm} and \hat{M} , operators chosen to act multiplicatively on the horizon wave-function. The specific charge α is viewed as a parameter.

Without going into too many details (for more information, the reader is referred to [13, 14]), in this case a HWF can be expressed for each of the two horizons. This is the case because the total energy can be expressed in terms of only R_+ , respectively R_- .

The probability densities for the particle to lie inside its own horizons of sizes $r = R_{\pm}$ can now be calculated as

$$\mathcal{P}_{<\pm}(r < R_{\pm}) = P_S(r < R_{\pm}) \mathcal{P}_H(R_{\pm}), \quad (15)$$

where the expressions for $P_S(r < R_{\pm})$ and $\mathcal{P}_H(R_{\pm})$ are calculated using the same method as their corresponding quantities from Eq. (8), respectively (9).

Finally, one can integrate the previous equation (the case with the upper signs) over all possible values of the horizon radius R_+ to find the probability for the particle described by the wave-function (2) to be a BH, namely

$$P_{\text{BH}+} = \int_{R_{\text{min}+}}^{\infty} \mathcal{P}_{<+}(r < R_+) dR_+. \quad (16)$$

The analogous quantity for R_- ,

$$P_{\text{BH}-} = \int_{R_{\text{min}-}}^{\infty} \mathcal{P}_{<-}(r < R_-) dR_-, \quad (17)$$

will instead be the probability that the particle lies further inside its inner horizon. It is already clear from these definitions that $P_{\text{BH}-} < P_{\text{BH}+}$, and it is only when $P_{\text{BH}-}$ is significantly high that one can say that both R_- and R_+ are physically realised. The expressions for the HWFs and their normalisations, along with more details about obtaining the above mentioned probabilities can be found in [13].

2.2.1. Inner Horizon of the Quantum Reissner-Nordström Black Holes

We shall now present our findings for the case $0 < \alpha \leq 1$, which classically possess at least one horizon. Once again, to determine the HWF and then calculate the probabilities for both the inner and outer horizon to exist, the classical relations (14) are lifted to the rank of equations for the operators \hat{R}_{\pm} and \hat{M} , which are chosen to act multiplicatively on the horizon wave-function.

Figure 4 shows $P_{\text{BH}+}$ and $P_{\text{BH}-}$ as functions of α for particle mass values above, equal to and below the Planck mass. The plot shows that $P_{\text{BH}+}$ stays very close to one for mass values larger than the Planck scale. When $m \sim m_p$ (when the width of the Gaussian wave-packet $\ell \sim \ell_p$), the probability starts to decrease below one as the specific charge increases to one. Note that this probability is not exactly zero even for values of the mass smaller than m_p . For instance, in the case $m = 0.5m_p$, corresponding to a width $\ell = 2\ell_p$ of the Gaussian wave-packet, $P_{\text{BH}+} \simeq 0.2$ for a considerable range of α values. It only decreases below 0.1 when α approaches one, therefore when the BH becomes maximally charged.

The situation is very different for the inner horizon. The same plot shows that the probability $P_{\text{BH}-}$ is approximately zero for small values of the charge-to-mass ratio and slowly increases with α . The larger the mass of the particle, the smaller

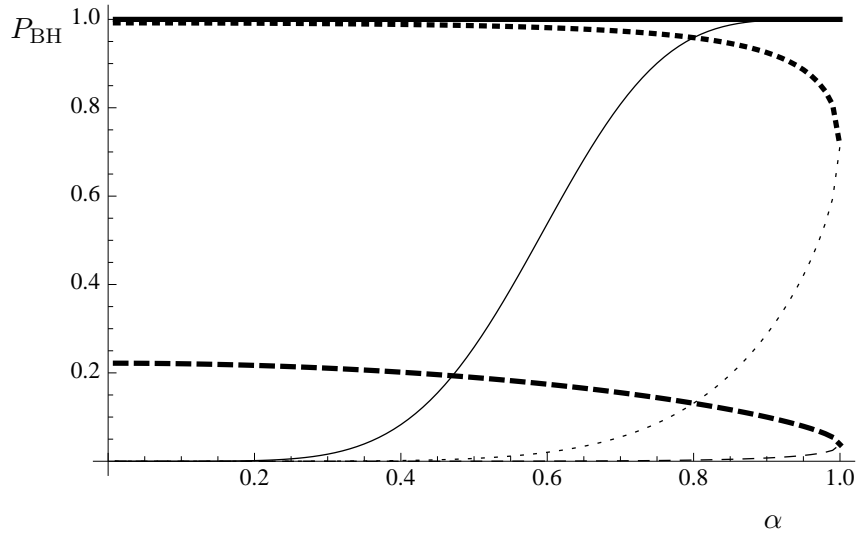


Fig. 4 – Probability $P_{\text{BH}+}$ in Eq. (16) for the particle to be a BH (thick lines) and $P_{\text{BH}-}$ in Eq. (17) for the particle to be inside its inner horizon (thin lines) as functions of α for $m = 2m_{\text{p}}$ (continuous line), $m = m_{\text{p}}$ (dotted line) and $m = 0.5m_{\text{p}}$ (dashed line). For $\alpha = 1$ the two probabilities merge.

the value of α for which the probability starts to become significant. What is very interesting is that for a considerable range of values of the specific charge, while $P_{\text{BH}+} \simeq 1$ thus making the object a BH, the probability for the inner horizon to exist is approximately zero.

The probabilities $P_{\text{BH}\pm}$ as functions of the mass m for constant values of the specific charge ($\alpha = 0.3, 0.8$ and 1) are shown in Fig. 5. It is found that the smaller the value of α , the smaller value of m at which the probability $P_{\text{BH}+}$ starts to increase from zero to one. The opposite is true when analyzing $P_{\text{BH}-}$. For $\alpha = 0.3$ for instance, it is only around $m \simeq 6m_{\text{p}}$ that both probabilities $P_{\text{BH}+}$ and $P_{\text{BH}-}$ have values close to one, while $P_{\text{BH}+}$ already increases to one around m_{p} . Therefore in the range from m_{p} to $6m_{\text{p}}$, the probability $P_{\text{BH}+} \simeq 1$ while $P_{\text{BH}-} \simeq 0$. This domain of values increases even more for smaller values of the specific charge, but it decreases to zero when the BH is maximally charged.

We therefore find a considerable parameter space for particle mass values (around the Planck scale) and $\alpha < 1$ in which

$$P_{\text{BH}+} \simeq 1 \quad \text{and} \quad P_{\text{BH}-} \simeq 0. \quad (18)$$

The existence of the outer horizon determines the fact that the particle is a BH, which we consider equivalent to $P_{\text{BH}+} \simeq 1$. The existence of an inner horizon at $r = R_-$ is important in light of the "mass inflation" instability and puzzling features of Cauchy horizons. Eq. (18) therefore means that the particle is a BH, but no such peculiarities

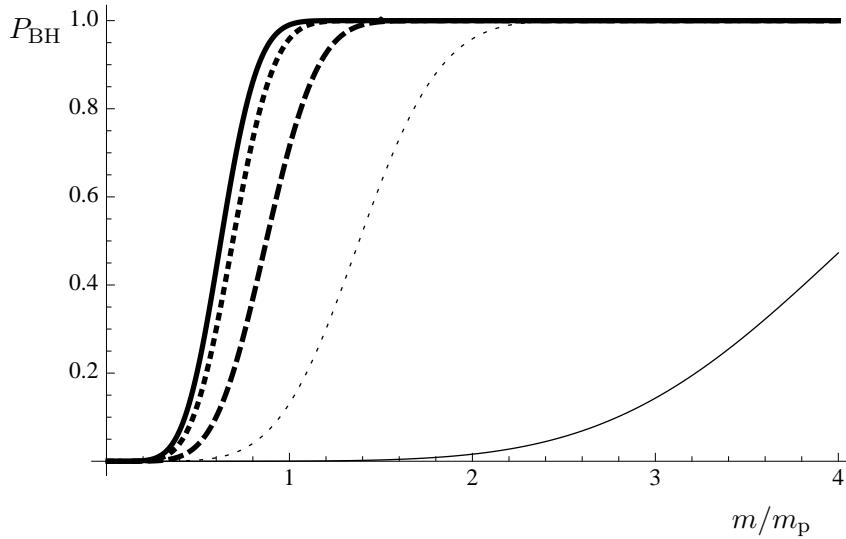


Fig. 5 – Probability $P_{\text{BH}+}$ in Eq. (16) for the particle to be a BH (thick lines) and $P_{\text{BH}-}$ in Eq. (17) for the particle to be inside its inner horizon (thin lines) as functions of the mass for $\alpha = 0.3$ (continuous line), $\alpha = 0.8$ (dotted line) and $\alpha = 1$ (dashed line). For $\alpha = 1$ thick and thin dashed lines overlap.

are expected.

We should not leave this section before stating that also in this case one naturally recovers an effective generalised uncertainty principle like in Section 2.1.1, in the sense that the dependence on the momentum Δp is the same, but with different pre-factors.

2.2.2. Superextremal black holes. Notes on the Cosmic Censorship Conjecture

In the General Relativistic treatment, the maximum value of the specific electric charge is one. This way, the cosmic censorship conjecture forbids *a priori* the existence of naked singularities. In this section we will go one step forward, in what we consider to be a very interesting mathematical exercise, and we will investigate the regime of overcharged sources, represented by values of the specific charge in the range $\alpha > 1$. It will be interesting to see if QM affects the predictions summarised above.

The main issue in the $\alpha > 1$ regime is that the operators \hat{R}_{\pm} are not Hermitian. One option would be to just say that there are no observables which correspond to \hat{R}_{\pm} in the regime $\alpha > 1$. However, let us make a simple choice, which allows us to proceed and probe the classically forbidden region. Let's take the real parts of the multiplicative operators \hat{R}_{\pm} , which are certainly Hermitian, to correspond to quantum observables. With this choice, the modulus squared of the HWF is given by

(for further details please consult [14])

$$|\psi_{\text{H}}(R)|^2 = \mathcal{N}^2 \exp \left\{ -\frac{2 - \alpha^2}{\alpha^4} \frac{m_{\text{p}}^2 R^2}{\Delta^2 \ell_{\text{p}}^2} \right\}. \quad (19)$$

We point out that for $\alpha > 1$, only one HWF exists and R replaces both R_+ and R_- . This HWF is still normalizable in the scalar product (6), if R belongs to the real axis and the specific charge lies in the range

$$1 < \alpha^2 < 2. \quad (20)$$

We, therefore, conclude that no normalisable quantum state with $\alpha^2 > 2$ is allowed, or that there is an obstruction that prevents the system from crossing $\alpha^2 = 2$.

As a quick check that our using the real part of the multiplicative operators \hat{R}_{\pm} (later denoted by \hat{R}) to correspond to quantum observables is not too far fetched, we calculated the expectation value of this operator and showed that what we find in the limit $\alpha \searrow 1$ equals the expectation value of \hat{R}_{\pm} when $\alpha \nearrow 1$:

$$\lim_{\alpha \searrow 1} \langle \hat{R} \rangle = \frac{4\ell_{\text{p}}^2/\ell}{2 + e\sqrt{\pi} \operatorname{erf}(1)} = \lim_{\alpha \nearrow 1} \langle \hat{R}_{\pm} \rangle. \quad (21)$$

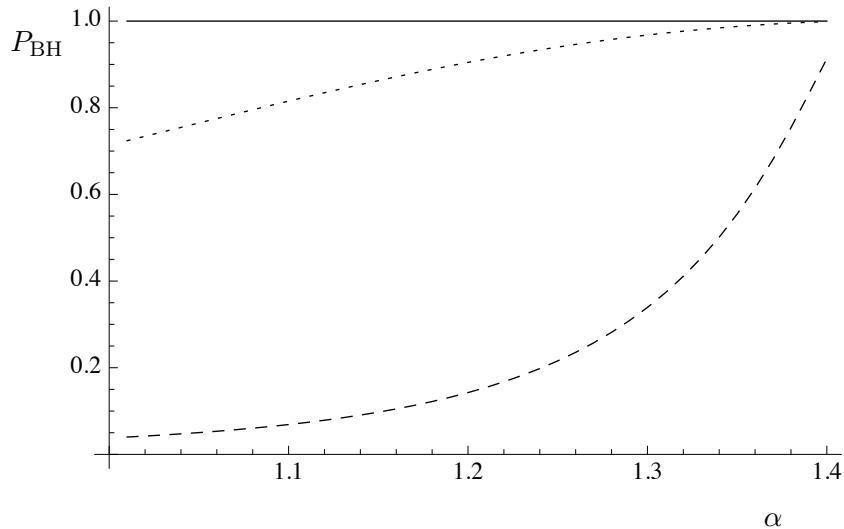


Fig. 6 – P_{BH} as a function of α for $m = 2m_{\text{p}}$ (solid line), $m = m_{\text{p}}$ (dotted line) and $m = 0.5m_{\text{p}}$ (dashed line). Cases with $m \gg m_{\text{p}}$ are not plotted since they behave the same as $m = 2m_{\text{p}}$, i.e. an object with $1 < \alpha^2 < 2$ must be a BH.

Using Eq. (16), we proceed to calculate the probability P_{BH} that the particle is a BH for α in the allowed superextremal range (20). We notice in Fig. 6 that, for a particle mass above the Planck scale, P_{BH} is approximately one throughout the

entire range of α (thus extending a similar result that holds for $\alpha < 1$). Moreover, even for m significantly below m_p , P_{BH} approaches one in the limit $\alpha^2 \rightarrow 2$. We need to emphasize that for small m , $P_{\text{BH}} \ll 1$ is related to $\ell \gg \langle \hat{R} \rangle$, and the system is thus dominated by quantum fluctuations in the source's position well below the Planck scale. On the other end, both $\langle \hat{R} \rangle$ and ΔR blow up in the limit $\alpha^2 = 2$, therefore the superextremal configurations with a significant probability of being BHs contain strong quantum fluctuations in the horizon's size.

Let us emphasise again that, in order to achieve the above results, we had to continue the HWF and the operators that are straightforwardly defined for $\alpha < 1$ into the superextremal regime. This choice is not necessarily unique, one might wonder whether different options would lead to very different outcomes. Although we have not performed a full survey, we should note that we were able to ensure the continuity of expectation values across $\alpha = 1$, like in Eq. (21).

3. CONCLUSIONS

The HWF formalism was introduced as a tool to allow one to effectively describe the emergence of horizons in localised Quantum Mechanical systems. We applied the HWF formalism to particles described by spherically symmetric Gaussian wave-functions, and we obtained non-vanishing probabilities for the particles to be BHs when their masses are larger than about $m_p/4$ (for all the details, see Refs. [7, 9, 13, 14]). This shows that, contrary to the case of a purely general relativistic treatment when there is strict threshold at the Planck scale, QM effects do allow BH formation even below the m_p . Of course as the particle mass decreases more and more below the Planck scale, the probability for that QM wave-packet to be a BH is smaller until it vanishes around $m_p/4$. We want to draw our reader's attention that in one of the articles cited above, Ref. [9], we reached similar conclusions for the case of the collision between two QM wave-packets.

In the case of electrically charged BHs with $\alpha \leq 1$, we found that in a quantum regime (let's say $m \lesssim 10m_p$) quantum fluctuations around the inner horizon are strong enough to prevent the instability expected according to the semiclassical analysis [13]. The probability for any instability to occur will be as small as $P_{\text{BH-}}$. QM effects also allow us to continuously go into the region of superextremal BHs with $\alpha > 1$. This means that overcharged quantum BHs might be possible [14].

We therefore find that the HWF formalism supports the existence of a minimum BH mass in a genuinely QM fashion, since it produces negligible probabilities for particles with masses much smaller than m_p to be BHs, rather than giving a sharp value above which the transition from particles to BHs occurs. Further, the description of BHs that the HWF formalism entails is shown to be compatible with GUPs,

since it yields the same kind of uncertainty relation in phase space.

Acknowledgements. The authors would like to acknowledge the extensive contribution that Dr. Dejan Stojkovic of the State University of New York at Buffalo had to the development of this work. R.C. was supported in part by the INFN grant FLAG.

REFERENCES

1. J.R. Oppenheimer and H. Snyder, *Phys. Rev.* **56**, 455 (1939).
2. J.R. Oppenheimer and G.M. Volkoff, *Phys. Rev.* **55**, 374 (1939).
3. P.S. Joshi, "Gravitational Collapse and Spacetime Singularities," Cambridge Monographs on Mathematical Physics (Cambridge, 2007).
4. K.S. Thorne, "Nonspherical Gravitational Collapse: A Short Review," in *J.R. Klauder, Magic Without Magic*, San Francisco (1972), 231.
5. E. Greenwood and D. Stojkovic, *JHEP* 032P 0408.
6. R. Casadio, "Localised particles and fuzzy horizons: A tool for probing Quantum Black Holes," arXiv:1305.3195.
7. R. Casadio and F. Scardigli, *Eur. Phys. J. C* **74**, 2685 (2014).
8. R. Casadio, *Eur. Phys. J. C* **75**, 160 (2015).
9. R. Casadio, O. Micu and F. Scardigli, *Phys. Lett. B* **732**, 105 (2014).
10. R. Casadio, A. Giugno, O. Micu and A. Orlandi, *Phys. Rev. D* **90**, 084040 (2014).
11. R. Casadio, A. Giugno and A. Orlandi, *Phys. Rev. D* **91**, 124069 (2015).
12. J. E. Wang, E. Greenwood and D. Stojkovic, *Phys. Rev. D* **80**, 124027 (2009).
13. R. Casadio, O. Micu and D. Stojkovic, *JHEP* **1505**, 096 (2015).
14. R. Casadio, O. Micu and D. Stojkovic, *Phys. Lett. B* **747**, 68 (2015).
15. E. Poisson and W. Israel, *Phys. Rev. D* **41**, 1796 (1990).
16. V. I. Dokuchaev, *Class. Quant. Grav.* **31**, 055009 (2014).
17. E. Brown and R. B. Mann, *Phys. Lett. B* **694**, 440 (2011).
18. E. G. Brown, R. B. Mann and L. Modesto, *Phys. Rev. D* **84**, 104041 (2011).